J. Fluid Mech. (2002), *vol.* 461, *pp.* 343–364.
DOI: 10.1017/S002211200200842X Printed in the United Kingdom

Scattering of oblique waves in a two-layer fluid

By C. M. LINTON AND J. R. CADBY

Department of Mathematical Sciences, Loughborough University, Leicestershire LE11 3TU, UK

(Received 17 September 2001)

We consider problems based on linear water wave theory concerning the interaction of oblique waves with horizontal cylinders in a fluid consisting of a layer of finite depth bounded above by a free surface and below by an infinite layer of fluid of greater density. For such a situation time-harmonic waves can propagate with two different wavenumbers K and k. The particular problems of wave scattering by a horizontal circular cylinder in either the upper or lower layer are solved using multipole expansions.

1. Introduction

The propagation of waves in a two-layer fluid with both a free surface and an interface (in the absence of any obstacles) was first investigated by Stokes (1847) and a description of some of the types of wave motion which can occur is given in Lamb (1932, Art. 231). However, until recently, very little work has been done on wave/structure interactions in two-layer fluids.

With the free surface approximated by a rigid lid Sturova (1994*a*) studied the radiation of waves by an oscillating cylinder which is moving uniformly in a direction perpendicular to its axis. Sturova (1999) later considered the radiation and scattering problem for a cylinder in both a two- and a three-layer fluid bounded above and below by rigid horizontal walls. For the three-layer case the middle layer was linearly stratified representing a smooth pycnocline. Using the method of multipoles Sturova was able to calculate the hydrodynamic characteristics of the cylinder. Gavrilov, Ermanyuk & Sturova (1999) also investigated the effects of a smooth pycnocline on wave scattering, again for a horizontal circular cylinder where the fluid is bounded above and below by rigid walls. Their paper included a comparison between theoretical and experimental results, with reasonable qualitative agreement but notable quantitative disagreement.

A simpler approach is to assume that the pycnocline is very thin and to model the interface between the two fluids as a sharp discontinuity between layers of constant density. We will make this simplifying assumption here, but in contrast to the papers cited above, we will assume that the upper surface of the upper fluid is free, and apply the linear free-surface boundary condition there. In the absence of obstacles, the appropriate dispersion relation for such a two-layer fluid has two solutions for a given frequency (Lamb 1932, Art. 231). One of these solutions corresponds to waves where the majority of the disturbance is close to the free surface and the other to waves on the interface between the two fluid layers.

When a wave is scattered by an obstacle there is the possibility that the wave energy will be transferred between the two modes. Linton & McIver (1995, hereafter referred to as LM) developed a general theory for two-dimensional wave scattering by horizontal cylinders in an infinitely deep two-layer fluid, and calculated the amount of energy that was converted from one wavenumber to the other for the case of circular cylinders in either the upper or lower fluid layer. They also systematically derived the reciprocity relations that exist between the various hydrodynamic characteristics of the cylinders. It is well-known that a circular cylinder submerged in an infinitely deep uniform fluid reflects no wave energy, and it was shown in LM that this is also true for a cylinder in the lower layer of a two-layer fluid (though when the cylinder is in the upper layer this is no longer the case).

Work on three-dimensional scattering can be found in Yeung & Nguyen (1999) and Cadby & Linton (2000). In the former work an integral equation technique was employed to solve radiation and diffraction problems for a rectangular barge in finite depth, whereas in the latter paper multipole expansions were used to solve problems involving submerged spheres in infinite depth. The symmetry relations for the added-mass and damping matrices and an analogue to the Haskind relations were given in Yeung & Nguyen (1999); a more complete derivation of reciprocity relations in three-dimensional scattering in two-layer fluids can be found in Cadby & Linton (2000).

Other notable work on wave/structure interaction in two-layer fluids includes Sturova (1994*b*), in which a hybrid element approach was used to compute added mass and damping coefficients for an elliptic cylinder in the lower layer of a two-layer fluid, and Zilman & Miloh (1995) and Zilman, Kagan & Miloh (1996), in which the effects of a shallow layer of fluid mud on the hydrodynamics of floating bodies was analysed. In Barthélemy, Kabbaj & Germain (2000) the scattering of surface waves by a step bottom in a two-layer fluid was considered. This problem is of particular interest in understanding how tides are scattered at the continental shelf break. A WKBJ technique, which approximates the solution by simple travelling waves locally, was employed to find the reflection and transmission coefficients of the surface waves past the step and the proportion of the surface motion transferred to the interface.

In this paper we extend the work of LM to the case of oblique wave incidence and use multipole expansions to solve scattering problems involving horizontal circular cylinders. For the case of an incident wave on the interface we find some surprising results. There is a critical angle (defined by the density ratio between the two fluids), and for an incident wave angle above this no energy is transferred to the free surface in the scattering process. For angles less than the critical angle, then energy transfer only occurs at high enough frequencies. Within the regime where no energy transfer takes place we find the phenomenon of zero transmission (and therefore total reflection) at particular frequencies. The general problem of oblique wave incidence in two-layer fluids is formulated in § 2 and then the case of a cylinder in the lower layer is treated in § 3 and a cylinder in the upper layer is treated in § 4.

2. Formulation

Cartesian coordinates are chosen such that the (x, y)-plane coincides with the undisturbed interface between the two fluids. The z-axis points vertically upwards with $z = 0$ as the interface and $z = d > 0$ as the free surface. Under the usual assumptions of linear water wave theory we can define a velocity potential in the form

$$\Phi(x, y, z, t) = Re\{\phi(x, z)\mathrm{e}^{\mathrm{i}ly}\mathrm{e}^{-\mathrm{i}\omega t}\} \tag{2.1}$$

and since Φ is harmonic, ϕ must satisfy the modified Helmholtz equation

$$(\nabla^2_{xz} - l^2)\phi = 0. \tag{2.2}$$

The upper fluid, $0 < z < d$, will be referred to as region I, whilst the lower fluid, $z < 0$, will be referred to as region II. The potential in the upper fluid (of density ρ^I) will be denoted by ϕ^I and that in the lower fluid (of density $\rho^{II} > \rho^I$) by ϕ^{II}. If we define $\rho = \rho^I/\rho^{II} (< 1)$ then the linearized boundary conditions on the interface and free surface are

$$\phi^I_z = \phi^{II}_z \quad \text{on} \quad z = 0, \tag{2.3}$$

$$\rho(\phi^I_z - K\phi^I) = \phi^{II}_z - K\phi^{II} \quad \text{on} \quad z = 0, \tag{2.4}$$

$$\phi^I_z = K\phi^I \quad \text{on} \quad z = d, \tag{2.5}$$

where $K = \omega^2/g$, g being the acceleration due to gravity. The boundary conditions (2.3) and (2.4) represent the continuity of normal velocity and pressure at the interface respectively.

Within this framework progressive waves take the form (up to an arbitrary multiplicative constant)

$$\phi^I = \exp(\pm \mathrm{i}x\sqrt{u^2 - l^2})((u + K)\mathrm{e}^{u(z-d)} + (u - K)\mathrm{e}^{-u(z-d)}), \tag{2.6}$$

$$\phi^{II} = \exp(\pm \mathrm{i}x\sqrt{u^2 - l^2})\mathrm{e}^{uz}((u + K)\mathrm{e}^{-ud} - (u - K)\mathrm{e}^{ud}), \tag{2.7}$$

where u satisfies the dispersion relation

$$(u - K)(K(\sigma + \mathrm{e}^{-2ud}) - u(1 - \mathrm{e}^{-2ud})) = 0 \tag{2.8}$$

in which $\sigma = (1 + \rho)/(1 - \rho)$. It follows that either $u = K$ or $u = k$ where

$$K(\sigma + \mathrm{e}^{-2kd}) = k(1 - \mathrm{e}^{-2kd}). \tag{2.9}$$

This equation has exactly one positive root k, which is always greater than K.

For the case $u = K$, progressive waves are thus of the form

$$\phi^I = \phi^{II} = \mathrm{e}^{\pm \mathrm{i}\beta x}\mathrm{e}^{Kz}, \tag{2.10}$$

where $\beta = \sqrt{K^2 - l^2}$ and we clearly must have $K > l$. For the case $u = k$ on the other hand, we have

$$\phi^I = \mathrm{e}^{\pm \mathrm{i}bx} g(z), \quad \phi^{II} = \mathrm{e}^{\pm \mathrm{i}bx}\mathrm{e}^{kz}, \tag{2.11}$$

where $b = \sqrt{k^2 - l^2}$ and

$$g(z) = \frac{K\sigma - k}{K(\sigma - 1)}\mathrm{e}^{kz} + \frac{K - k}{K(\sigma - 1)}\mathrm{e}^{-kz}. \tag{2.12}$$

In this case we require $k > l$ for the waves to exist. A general scattered potential thus has the far-field behaviour described by

$$\phi^I \sim A^\pm \mathrm{e}^{\pm \mathrm{i}\beta x}\mathrm{e}^{Kz} + B^\pm \mathrm{e}^{\pm \mathrm{i}bx} g(z) + C^\pm \mathrm{e}^{\mp \mathrm{i}\beta x}\mathrm{e}^{Kz} + D^\pm \mathrm{e}^{\mp \mathrm{i}bx} g(z), \tag{2.13}$$

$$\phi^{II} \sim A^\pm \mathrm{e}^{\pm \mathrm{i}\beta x}\mathrm{e}^{Kz} + B^\pm \mathrm{e}^{\pm \mathrm{i}bx}\mathrm{e}^{kz} + C^\pm \mathrm{e}^{\mp \mathrm{i}\beta x}\mathrm{e}^{Kz} + D^\pm \mathrm{e}^{\mp \mathrm{i}bx}\mathrm{e}^{kz}, \tag{2.14}$$

as $x \to \pm\infty$, for which a convenient shorthand is

$$\phi \sim \{A^-, B^-, C^-, D^-; A^+, B^+, C^+, D^+\}. \tag{2.15}$$

An incident plane wave ϕ_{inc} of wavenumber K making an angle α_{inc} ($0 \leqslant \alpha_{\mathrm{inc}} < \frac{1}{2}\pi$) with the positive x-axis has the form (in both layers)

$$\phi_{\mathrm{inc}} = \mathrm{e}^{\mathrm{i}Kx\cos\alpha_{\mathrm{inc}}}\mathrm{e}^{Kz}. \tag{2.16}$$

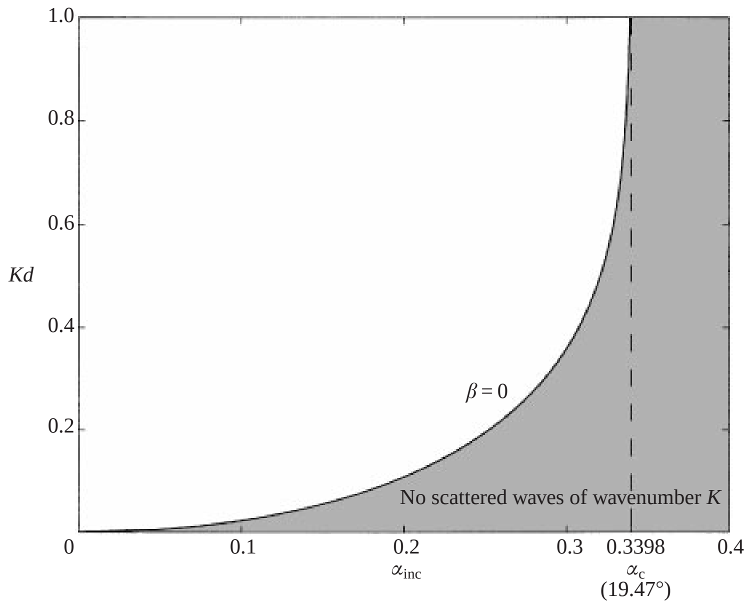

FIGURE 1. Cut-off frequency $K_c d$ due to an incident wave of wavenumber k; $\rho = 0.5$.

In this case

$$l = K \sin\alpha_{\text{inc}}, \quad \beta = K \cos\alpha_{\text{inc}}, \quad b = \sqrt{k^2 - K^2 \sin^2\alpha_{\text{inc}}}. \tag{2.17}$$

We know that b is real since $k > K$ and so scattered waves of wavenumber k will exist for all values of K and all angles α_{inc}. The angle α_k of the scattered waves of wavenumber k is given by

$$\tan\alpha_k = \frac{l}{b} = \frac{K \sin\alpha_{\text{inc}}}{\sqrt{k^2 - K^2 \sin^2\alpha_{\text{inc}}}}. \tag{2.18}$$

Since $b > \beta$ we know that $\tan\alpha_k < \tan\alpha_{\text{inc}}$ and hence $|\alpha_k| < \alpha_{\text{inc}}$.

An incident plane wave of wavenumber k making an angle α_{inc} with the positive x-axis is given by

$$\phi^I_{\text{inc}} = \mathrm{e}^{\mathrm{i}kx\cos\alpha_{\text{inc}}} g(z), \quad \phi^{II}_{\text{inc}} = \mathrm{e}^{\mathrm{i}kx\cos\alpha_{\text{inc}}} \mathrm{e}^{kz}. \tag{2.19}$$

In this case

$$l = k \sin\alpha_{\text{inc}}, \quad \beta = \sqrt{K^2 - k^2 \sin^2\alpha_{\text{inc}}}, \quad b = k \cos\alpha_{\text{inc}}. \tag{2.20}$$

For a given angle α_{inc} there maybe a value of K for which $K = k \sin\alpha_{\text{inc}}$ and thus $\beta = 0$. We will call this the cut-off frequency and denote it by K_c. For $K > K_c$ we have real β and so waves of wavenumber K will propagate in the fluid. When $K < K_c$, however, β will be imaginary, corresponding to an evanescent mode, and hence we have no propagating waves of wavenumber K. From the dispersion relation (2.9) we have

$$K_c d = \tfrac{1}{2} \sin\alpha_{\text{inc}} \ln\left(\frac{1 + \sin\alpha_{\text{inc}}}{1 - \sigma \sin\alpha_{\text{inc}}}\right). \tag{2.21}$$

Figure 1 shows the cut-off frequency $K_c d$, plotted against incident wave angle, for a density ratio of $\rho = 0.5$ ($\sigma = 3$). There is a critical angle α_c, given by $\sin^{-1}(1/\sigma)$, such that as $\alpha_{\rm inc} \to \alpha_{\rm c}$ we have $K_{\rm c}d \to \infty$ and for $\alpha_{\rm inc} > \alpha_{\rm c}$ there are no propagating waves of wavenumber K for any frequency. When they do exist, the angle α_K of the scattered waves of wavenumber K is given by

$$\tan\alpha_K = \frac{k\sin\alpha_{\rm inc}}{\sqrt{K^2 - k^2\sin^2\alpha_{\rm inc}}}, \tag{2.22}$$

and $|\alpha_K| > \alpha_{\rm inc}$.

Relations between the various hydrodynamic quantities that arise in scattering problems can be obtained by using Green's theorem. The approach is almost identical to that described in LM and the formulas derived in that paper (equations (2.19)–(2.56)) for the case of normal incidence carry over to the oblique incidence case, except that now $J = J_k/J_K$ where

$$J_K = \mathrm{i}\beta\left(\frac{1}{K} + 2\rho\int_0^d \mathrm{e}^{2Kz}\mathrm{d}z\right), \quad J_k = \mathrm{i}b\left(\frac{1}{k} + 2\rho\int_0^d [\mathrm{g}(z)]^2\mathrm{d}z\right). \tag{2.23}$$

The scattering of an incident wave of wavenumber K can be characterized by

$$\phi_K \sim \{R_K, r_K, 1, 0; T_K, t_K, 0, 0\}, \tag{2.24}$$

where R_K and r_K are the reflection coefficients, and T_K and t_K are the transmission coefficients of wavenumbers K and k, respectively, and we have

$$|R_K|^2 + |T_K|^2 + J(|r_K|^2 + |t_K|^2) = 1. \tag{2.25}$$

For an incident wave of wavenumber k the velocity potential is characterized by

$$\phi_k \sim \{R_k, r_k, 0, 1; T_k, t_k, 0, 0\}, \tag{2.26}$$

and

$$|R_k|^2 + |T_k|^2 + J(|r_k|^2 + |t_k|^2) = J. \tag{2.27}$$

It is convenient to define energies as follows:

$$E_K^R = |R_K|^2, \quad E_K^T = |T_K|^2, \quad E_K^r = J|r_K|^2, \quad E_K^t = J|t_K|^2, \tag{2.28}$$

$$E_k^R = |R_k|^2/J, \quad E_k^T = |T_k|^2/J, \quad E_k^r = |r_k|^2, \quad E_k^t = |t_k|^2. \tag{2.29}$$

The energy relations (2.25) and (2.27) then become

$$E_j^R + E_j^T + E_j^r + E_j^t = 1, \quad j = k \quad \text{or} \quad K. \tag{2.30}$$

This equation was used as a numerical check on all results obtained for the reflection and transmission coefficients.

Equation (2.30) relates different far-field quantities that arise in the same scattering problem. Many of the other relations derived in LM relate quantities from different problems (for example, $E_K^R + E_K^T = E_k^r + E_k^t$). These relations only apply to oblique scattering when the value of l is the same for both problems. For example, say we wish to relate a scattering problem with potential ϕ_K and angle of incidence $\alpha_{\rm inc}^K$ to a problem with potential ϕ_k and angle $\alpha_{\rm inc}^k$. If we assign a value to $\alpha_{\rm inc}^K$ then the angle $\alpha_{\rm inc}^k$ is given by

$$\alpha_{\rm inc}^k = \sin^{-1}\left(\frac{K}{k}\sin\alpha_{\rm inc}^K\right) \tag{2.31}$$

and since $k > K$ there will always be an angle $\alpha_{\rm inc}^k$. However, unlike the normal incidence relations, we can only relate the results between the two problems at one particular frequency. (Or alternatively, the angle of incidence for the related problem depends on the frequency.) If we assign α_{inc}^k a value then

$$\alpha_{\text{inc}}^K = \sin^{-1}\left(\frac{k}{K}\sin\alpha_{\text{inc}}^k\right). \tag{2.32}$$

When $K < K_c$ or when $\alpha_{\text{inc}}^k > \alpha_c$ we will not be able to use such relations.

3. Cylinder in the lower fluid

A horizontal circular cylinder of radius a has its axis at $z = f < 0$ and its generator runs parallel to the y-axis. Polar coordinates (r, θ) are defined in the (x, z)-plane where

$$x = r\sin\theta \quad \text{and} \quad z = f - r\cos\theta. \tag{3.1}$$

Symmetric and antisymmetric multipoles, ϕ_n^s $(n \geqslant 0)$ and ϕ_n^a $(n \geqslant 1)$, respectively, are defined by

$$\phi_n^{Is} = (-1)^n \int_0^\infty \cosh nu \cos(lx\sinh u)[A_L(u)\mathrm{e}^{vz} + B_L(u)\mathrm{e}^{-vz}]\,\mathrm{d}u, \tag{3.2}$$

$$\phi_n^{IIs} = K_n(lr)\cos n\theta + (-1)^n \int_0^\infty \cosh nu \cos(lx\sinh u)\mathrm{e}^{vz}C_L(u)\,\mathrm{d}u, \tag{3.3}$$

$$\phi_n^{Ia} = (-1)^{n+1} \int_0^\infty \sinh nu \sin(lx\sinh u)[A_L(u)\mathrm{e}^{vz} + B_L(u)\mathrm{e}^{-vz}]\,\mathrm{d}u, \tag{3.4}$$

$$\phi_n^{IIa} = K_n(lr)\sin n\theta + (-1)^{n+1} \int_0^\infty \sinh nu \sin(lx\sinh u)\mathrm{e}^{vz}C_L(u)\,\mathrm{d}u, \tag{3.5}$$

where $v = l\cosh u$,

$$A_L(u) = K(1+\sigma)(v+K)\mathrm{e}^{v(f-2d)}/(v-K)h(v), \tag{3.6}$$

$$B_L(u) = K(1+\sigma)\mathrm{e}^{vf}/h(v), \tag{3.7}$$

$$C_L(u) = (v+K)[(v+K\sigma)\mathrm{e}^{-2vd} - v + K]\mathrm{e}^{vf}/(v-K)h(v), \tag{3.8}$$

and

$$h(v) = (v+K)\mathrm{e}^{-2vd} - v + K\sigma. \tag{3.9}$$

The functions ϕ_n^s and ϕ_n^a are singular solutions to the modified Helmholtz equation which satisfy all of the boundary conditions (including an outgoing radiation condition), except that on the body boundary. We note that the functions (3.6)–(3.8) are the same as (3.7)–(3.9) in LM with u replaced by $v(= l\cosh u)$.

From the dispersion relation we see that $h(k) = 0$, and hence the multipoles have poles at $u = \gamma_1$ and $u = \gamma_2$, where

$$l\cosh\gamma_1 = K \quad \text{and} \quad l\cosh\gamma_2 = k. \tag{3.10}$$

For $l > K$ there is only one pole at $u = \gamma_2$. The far-field form of the multipoles, in the lower fluid, is given by

$$\phi_n^{IIs} \sim (-1)^n \pi \mathrm{i}(C_L^{\gamma_1}\cosh n\gamma_1\,\mathrm{e}^{\pm \mathrm{i}\beta x}\mathrm{e}^{Kz} + C_L^{\gamma_2}\cosh n\gamma_2\,\mathrm{e}^{\pm \mathrm{i}bx}\mathrm{e}^{kz}), \tag{3.11}$$

$$\phi_n^{IIa} \sim \mp(-1)^n \pi(C_L^{\gamma_1}\sinh n\gamma_1\,\mathrm{e}^{\pm \mathrm{i}\beta x}\mathrm{e}^{Kz} + C_L^{\gamma_2}\sinh n\gamma_2\,\mathrm{e}^{\pm \mathrm{i}bx}\mathrm{e}^{kz}), \tag{3.12}$$

as $x \to \pm\infty$. Here $C_L^{\gamma_1}$ and $C_L^{\gamma_2}$ are the residues of $C_L(u)$ at $u = \gamma_1$ and $u = \gamma_2$, given by

$$C_L^{\gamma_1} = \frac{2K(1+\sigma)\mathrm{e}^{K(f-2d)}}{\beta(2\mathrm{e}^{-2Kd} - 1 + \sigma)} \tag{3.13}$$

and

$$C_L^{\gamma_2} = \frac{(k+K)\mathrm{e}^{kf}[(k+K\sigma)\mathrm{e}^{-2kd} - k + K]}{b(k-K)[(1-2d(k+K))\mathrm{e}^{-2kd} - 1]}. \tag{3.14}$$

The multipoles can be expanded in polar coordinates. If we put $X = -lr$ and $T = \exp(\mathrm{i}[\theta + \mathrm{i}u])$ in the well-known generating function (see, for example, Ursell 2001)

$$\exp[\tfrac{1}{2}X(T + T^{-1})] = \sum_{m=0}^{\infty} \tfrac{1}{2}\epsilon_m (T^m + T^{-m}) I_m(X), \tag{3.15}$$

where $\epsilon_0 = 1$, $\epsilon_m = 2$, $m \geqslant 1$, and then take the real and imaginary parts, the resulting expressions can be substituted into (3.3) and (3.5), using (3.1), to give

$$\phi_n^{IIs} = K_n(lr)\cos n\theta + \sum_{m=0}^{\infty} A_{nm}^s I_m(lr)\cos m\theta, \tag{3.16}$$

$$\phi_n^{IIa} = K_n(lr)\sin n\theta + \sum_{m=1}^{\infty} A_{nm}^a I_m(lr)\sin m\theta, \tag{3.17}$$

where

$$A_{nm}^s = \epsilon_m(-1)^{m+n} ⨍_0^{\infty} \cosh mu\, \cosh nu\, \mathrm{e}^{vf} C_L(u)\,\mathrm{d}u, \tag{3.18}$$

$$A_{nm}^a = 2(-1)^{m+n} ⨍_0^{\infty} \sinh mu\, \sinh nu\, \mathrm{e}^{vf} C_L(u)\,\mathrm{d}u. \tag{3.19}$$

Incident wavenumber K

Let us consider the case of an incident plane wave of wavenumber K making an angle α_{inc} with the positive x-axis, so that $l = K\sin\alpha_{\mathrm{inc}}$. The incident wave potential, (2.16), when expanded about $r = 0$ has the form (in both layers)

$$\phi_{\mathrm{inc}} = \mathrm{e}^{\mathrm{i}\beta x}\mathrm{e}^{Kz} = \mathrm{e}^{Kf}\sum_{m=0}^{\infty}\epsilon_m(-1)^m I_m(lr)(\cosh m\gamma\cos m\theta - \mathrm{i}\sinh m\gamma\sin m\theta), \tag{3.20}$$

where $\cosh\gamma = K/l = 1/\sin\alpha_{\mathrm{inc}}$. We write the velocity potential as

$$\phi_K = \phi_{\mathrm{inc}} + \sum_{m=0}^{\infty}(\alpha_m\phi_m^a + \beta_m\phi_m^s), \tag{3.21}$$

where α_m and β_m are unknown coefficients and α_0 is included for notational convenience. To solve for α_m and β_m we substitute the polar expansions of the multipoles and of the incident wave into (3.21) and apply the body boundary condition $\partial\phi_K/\partial r = 0$ on $r = a$. We then use the orthogonality of the trigonometric functions to obtain infinite systems of equations for the unknowns α_m and β_m which are

$$\alpha_n + Z_n \sum_{m=1}^{\infty} \alpha_m A^a_{mn} = 2\mathrm{i}(-1)^n Z_n \mathrm{e}^{Kf} \sinh n\gamma, \quad n = 1, 2, \ldots, \tag{3.22}$$

$$\beta_n + Z_n \sum_{m=0}^{\infty} \beta_m A^s_{mn} = \epsilon_n (-1)^{n+1} Z_n \mathrm{e}^{Kf} \cosh n\gamma, \quad n = 0, 1, \ldots, \tag{3.23}$$

where $Z_n = I'_n(la)/K'_n(la)$. These systems can be solved by truncation and in the computations presented below 5×5 systems were used. When the cylinder has submergence $f/a = -2$ this yields five-decimal-place accuracy whereas for $f/a = -1.1$ we have three-decimal-place accuracy.

The far-field form for ϕ_K, in the lower fluid layer, can be written as

$$\phi^{II}_K \sim \begin{cases} \mathrm{e}^{\mathrm{i}\beta x}\mathrm{e}^{Kz} + R_K \mathrm{e}^{-\mathrm{i}\beta x}\mathrm{e}^{Kz} + r_K \mathrm{e}^{-\mathrm{i}bx}\mathrm{e}^{kz}, & x \to -\infty, \\ T_K \mathrm{e}^{\mathrm{i}\beta x}\mathrm{e}^{Kz} + t_K \mathrm{e}^{\mathrm{i}bx}\mathrm{e}^{kz}, & x \to +\infty. \end{cases} \tag{3.24}$$

Using (3.21), (3.11) and (3.12) we can extract the reflection and transmission coefficients:

$$T_K = 1 + \pi C_L^{\gamma_1} \sum_{m=0}^{\infty} (-1)^m (-\alpha_m \sinh m\gamma_1 + \mathrm{i}\beta_m \cosh m\gamma_1), \tag{3.25}$$

$$R_K = \pi C_L^{\gamma_1} \sum_{m=0}^{\infty} (-1)^m (\alpha_m \sinh m\gamma_1 + \mathrm{i}\beta_m \cosh m\gamma_1), \tag{3.26}$$

$$t_K = \pi C_L^{\gamma_2} \sum_{m=0}^{\infty} (-1)^m (-\alpha_m \sinh m\gamma_2 + \mathrm{i}\beta_m \cosh m\gamma_2), \tag{3.27}$$

$$r_K = \pi C_L^{\gamma_2} \sum_{m=0}^{\infty} (-1)^m (\alpha_m \sinh m\gamma_2 + \mathrm{i}\beta_m \cosh m\gamma_2). \tag{3.28}$$

Incident wavenumber k

We now consider the case of an incident plane wave of wavenumber k making an angle α_{inc} with the positive x-axis, so that $l = k \sin \alpha_{\mathrm{inc}}$, and

$$\phi^{II}_{\mathrm{inc}} = \mathrm{e}^{\mathrm{i}bx}\mathrm{e}^{kz} = \mathrm{e}^{kf} \sum_{m=0}^{\infty} \epsilon_m (-1)^m I_m(lr)(\cosh m\gamma \cos m\theta - \mathrm{i} \sinh m\gamma \sin m\theta), \tag{3.29}$$

where $\cosh \gamma = k/l = 1/\sin \alpha_{\mathrm{inc}}$. The velocity potential ϕ_k for this scattering problem can again be expanded in multipoles using (3.21) and the equations for α_m and β_m are given by (3.22) and (3.23) as before, except that $\exp(Kf)$ must be replaced by $\exp(kf)$.

The far-field form for ϕ_k, in the lower fluid layer, can be written as

$$\phi^{II}_k \sim \begin{cases} \mathrm{e}^{\mathrm{i}bx}\mathrm{e}^{kz} + R_k \mathrm{e}^{-\mathrm{i}\beta x}\mathrm{e}^{Kz} + r_k \mathrm{e}^{-\mathrm{i}bx}\mathrm{e}^{kz}, & x \to -\infty, \\ T_k \mathrm{e}^{\mathrm{i}\beta x}\mathrm{e}^{Kz} + t_k \mathrm{e}^{\mathrm{i}bx}\mathrm{e}^{kz}, & x \to +\infty. \end{cases} \tag{3.30}$$

Using the far-field forms of the multipoles (3.11) and (3.12) with the expansion of ϕ_k we find that the expressions for R_k and r_k are the same as those for R_K and r_K given, respectively, by (3.26) and (3.28). For the transmission coefficients we have

$$T_k = \pi C_L^{\gamma_1} \sum_{m=0}^{\infty} (-1)^m(-\alpha_m \sinh m\gamma_1 + \mathrm{i}\beta_m \cosh m\gamma_1), \tag{3.31}$$

$$t_k = 1 + \pi C_L^{\gamma_2} \sum_{m=0}^{\infty} (-1)^m(-\alpha_m \sinh m\gamma_2 + \mathrm{i}\beta_m \cosh m\gamma_2). \tag{3.32}$$

For values of K less than the cut-off frequency K_c there are no waves of wavenumber K propagating to infinity and so $T_k = R_k = 0$.

Results

In figures 2 and 3 the reflection and transmission energies are shown for the case of a wave of wavenumber K (a free-surface mode) incident on a cylinder in the lower fluid layer. In all these plots the immersion depth f/a is -2, the depth of the upper fluid layer d/a is 2 and the density ratio ρ is 0.5. For a two-layer fluid consisting of fresh water and salt water the value of ρ would be around 0.97. The same qualitative features are observed for such a density ratio, but the effects of the interface are much smaller. The different curves correspond to different angles of incidence α_{inc}, which are 1.35, 1.4, 1.53 and 1.56 covering the range between about 75° and 89°. These values were chosen to illustrate the scattering behaviour when the angle of the incident wave approaches that of grazing ($\pi/2$). From figure 2 we see that as the angle of incidence increases, E_K^T decreases while E_K^R increases. This effect is also observed in the oblique scattering problem in a single-layer fluid. The transmission and reflection energies of the waves of wavenumber k, shown in figure 3, are small in comparison to those of the incident wavenumber K but show that there is some conversion of energy from one wavenumber to the other. As $\alpha_{\text{inc}} \to \pi/2$, for fixed K, we see that E_K^t, E_K^r and E_K^T tend to zero whereas E_K^R tends to unity. (For the single-layer problem Levine (1965) showed analytically, based on a low-order truncation of an infinite system, that $T_K \to 0$ while $R_K \to -1$ in this limit.) Computations show that as $\alpha_{\text{inc}} \to 0$ the results tend to those for normal incidence given in LM. In particular, as $\alpha_{\text{inc}} \to 0$ both E_K^R and E_K^r tend to zero.

The case of an incident wave of wavenumber k (an interfacial mode) is more interesting due to the presence of the cut-off frequency, below which no energy is converted from one wavenumber to the other. Figures 4 and 5 show the transmission and reflection energies for this case, when the immersion depth of the cylinder is $f/a = -1.1$ and we have the values $d/a = 2$ and $\rho = 0.5$, as before. Each plot shows the results obtained for four different angles α_{inc} of the incident wave close to the critical angle, 0.3, 0.32, 0.33, and 0.34 (17.19°–19.48°). When $\alpha_{\text{inc}} = 0.34$, which is greater than the critical angle $\alpha_c = 0.3398$ for the given parameter values, we have no waves of wavenumber K propagating in the fluid. For the remaining angles of incidence we have the following cut-off frequencies: $K_c a \approx 0.180$, 0.248 and 0.313. Only for frequencies greater than the cut-off will there be conversion of energy from one mode to the other. The transmission and reflection energies for the incident wavenumber are shown in figure 5. For a particular frequency just less than the cut-off there is zero transmission and full reflection of the incident wave. As α_{inc} increases the frequency at which this zero of transmission occurs increases and the spike from which it comes broadens. When $\alpha_{\text{inc}} = 0.34$ there are in fact two zeros of transmission, the second occurring at a higher frequency than those shown on the plot.

Further examples in which there are two zeros of transmission are shown in figures 6(a) and 6(b). Both these plots show the reflected energy of an incident wave

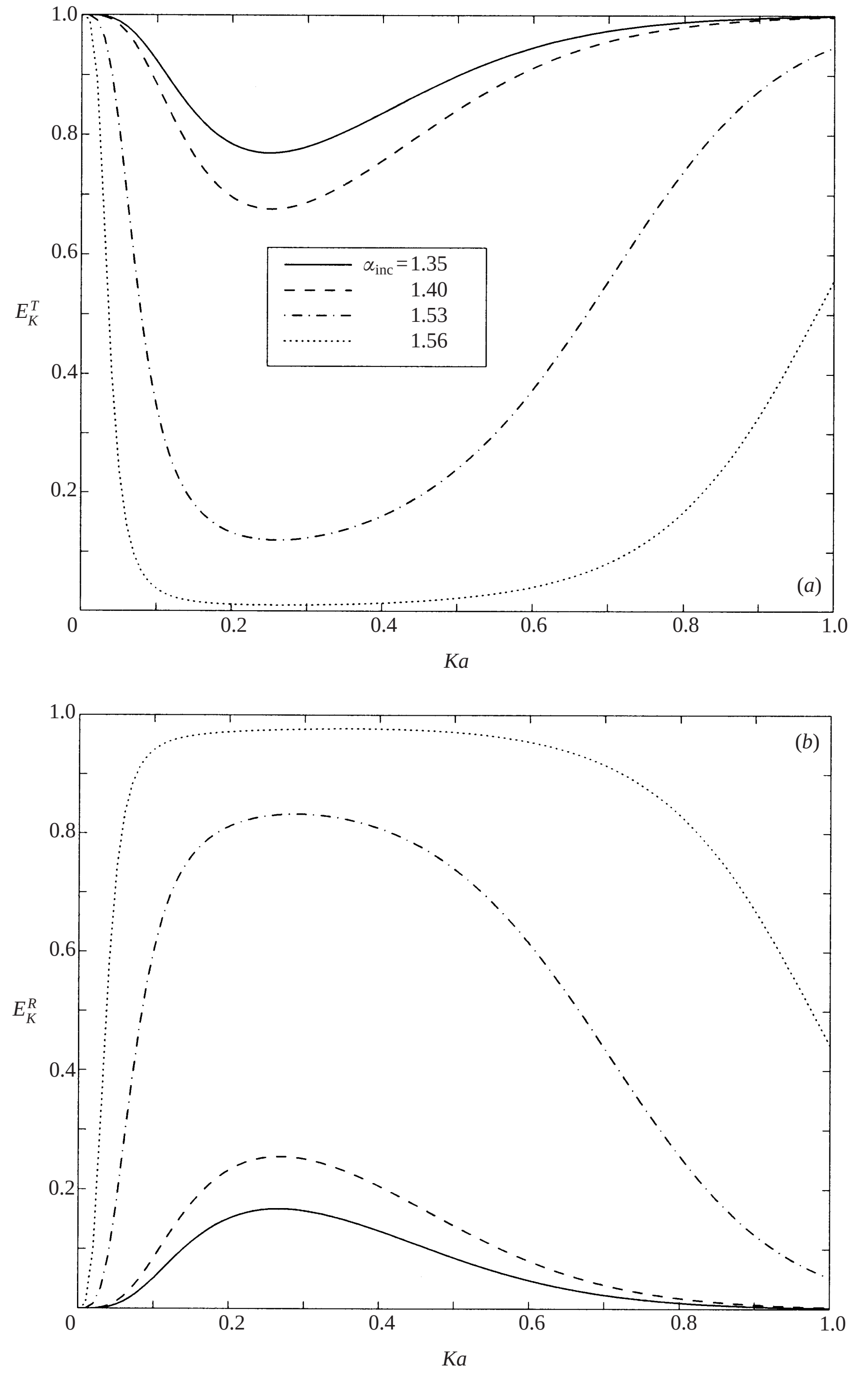

FIGURE 2. (a) Transmission and (b) reflection energies due to a wave of wavenumber K incident on a cylinder in the lower layer; $\rho = 0.5$, $d/a = 2.0$ and $f/a = -2.0$.

of wavenumber k where the values $\rho = 0.5$ and $\alpha_{inc} = 0.34$ have been used (since $\alpha_{inc} > \alpha_c$ in this case there is no energy converted to wavenumber K and hence a zero of transmission corresponds to total reflection at the incident wavenumber). In figure 6(a) the submergence of the cylinder is fixed at -1.95 and each curve

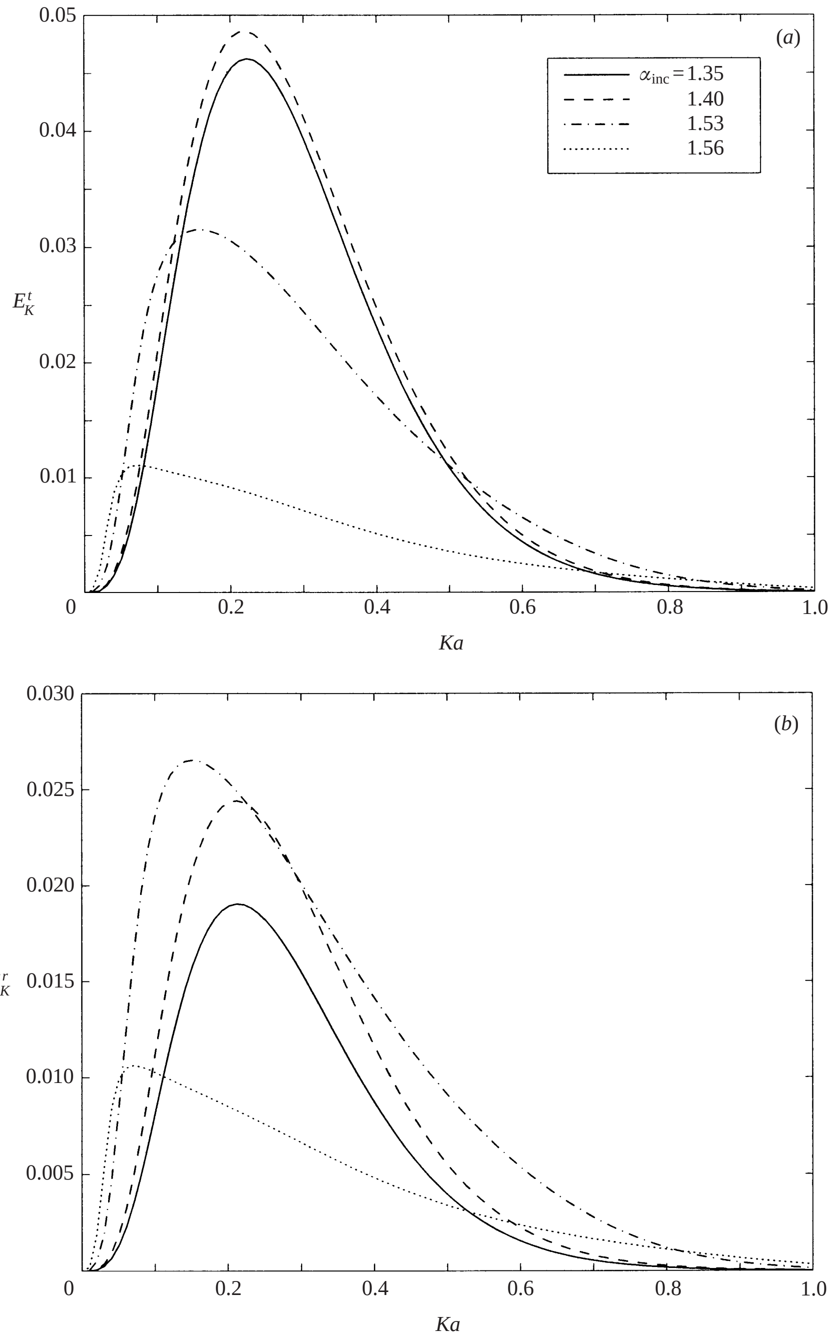

FIGURE 3. (a) Transmission and (b) reflection energies due to a wave of wavenumber K incident on a cylinder in the lower layer; $\rho = 0.5$, $d/a = 2.0$ and $f/a = -2.0$.

corresponds to a different depth of the upper fluid layer, $d/a = 2.7$, 2.5, 2.2 and 2. When $d/a \approx 2.5$ we see there is just one frequency of full reflection. As the depth of the upper fluid layer decreases this splits and gives two frequencies at which total reflection exists. A similar effect is observed when fixing the depth of the upper fluid and varying the submergence of the cylinder as in figure 6(b). The occurrence of zeros

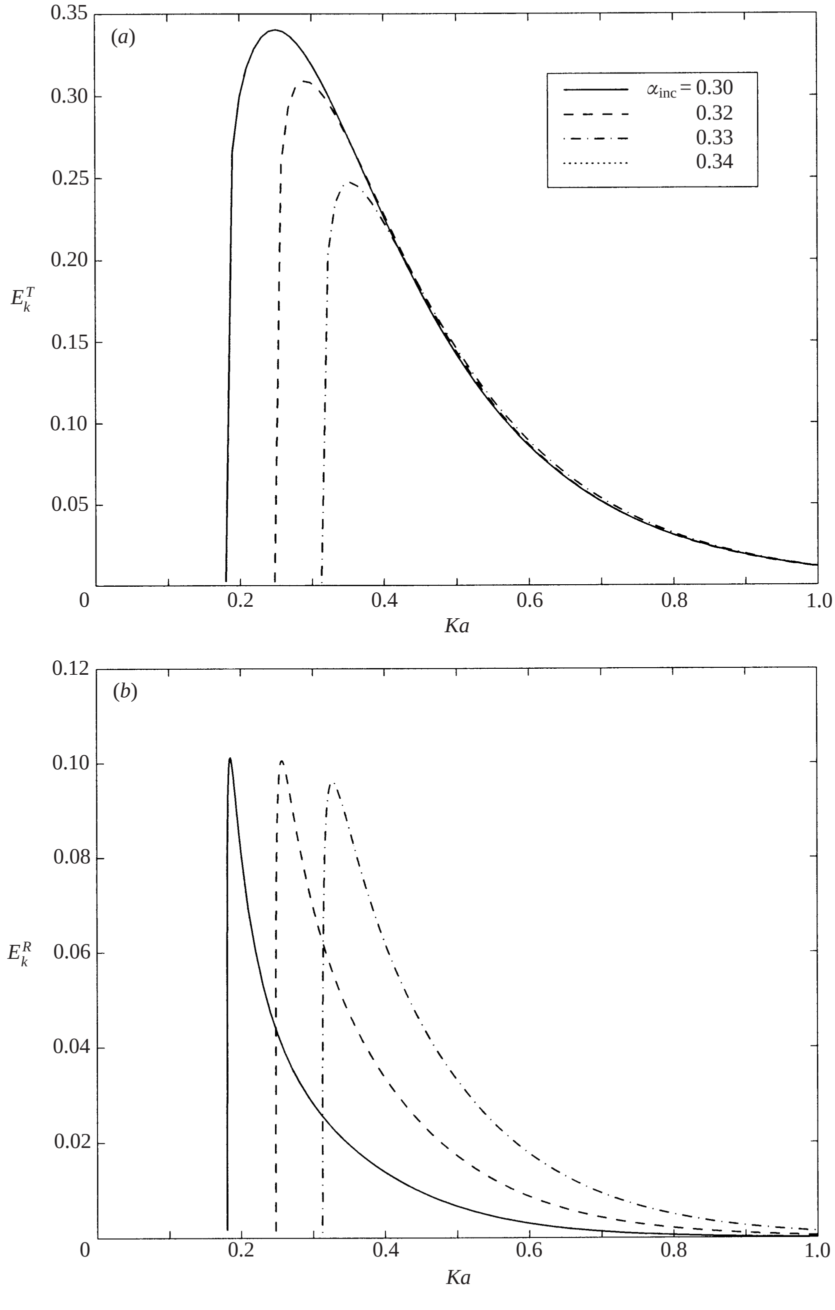

FIGURE 4. (*a*) Transmission and (*b*) reflection energies due to a wave of wavenumber k incident on a cylinder in the lower layer; $\rho = 0.5$, $d/a = 2.0$ and $f/a = -1.1$.

of transmission is somewhat surprising as normally incident waves on a cylinder in the lower fluid are completely transmitted at all frequencies (see LM); moreover, they do not occur in the single-layer oblique-incidence problem.

For the scattering of an incident wave k as $\alpha_{\text{inc}} \to \pi/2$ we find that $E_k^r \to 1$ while all the other energies tend to zero. As $\alpha_{\text{inc}} \to 0$ we again find that the results tend to those

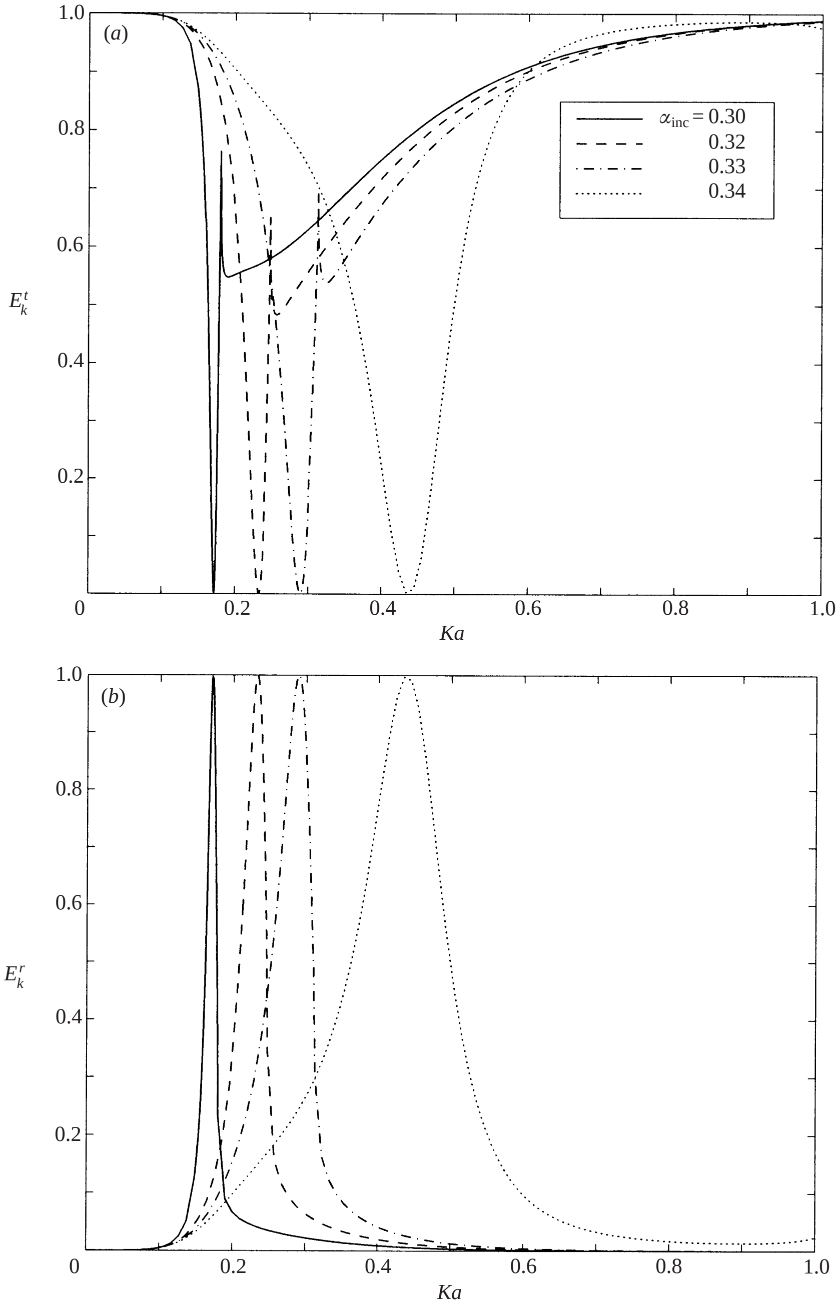

FIGURE 5. (a) Transmission and (b) reflection energies due to a wave of wavenumber k incident on a cylinder in the lower layer; $\rho = 0.5$, $d/a = 2.0$ and $f/a = -1.1$.

of the normal-incidence case. If we let $\rho \to 0$ in this problem then it can be shown that the multipoles defined by (3.3) and (3.5) go over to the equivalent single-layer multipoles for infinite depth (given in Linton & McIver 2001, for example). Thus by letting $\rho \to 0$ in the above analysis we recover the results for the scattering of oblique waves by a horizontal cylinder in deep water.

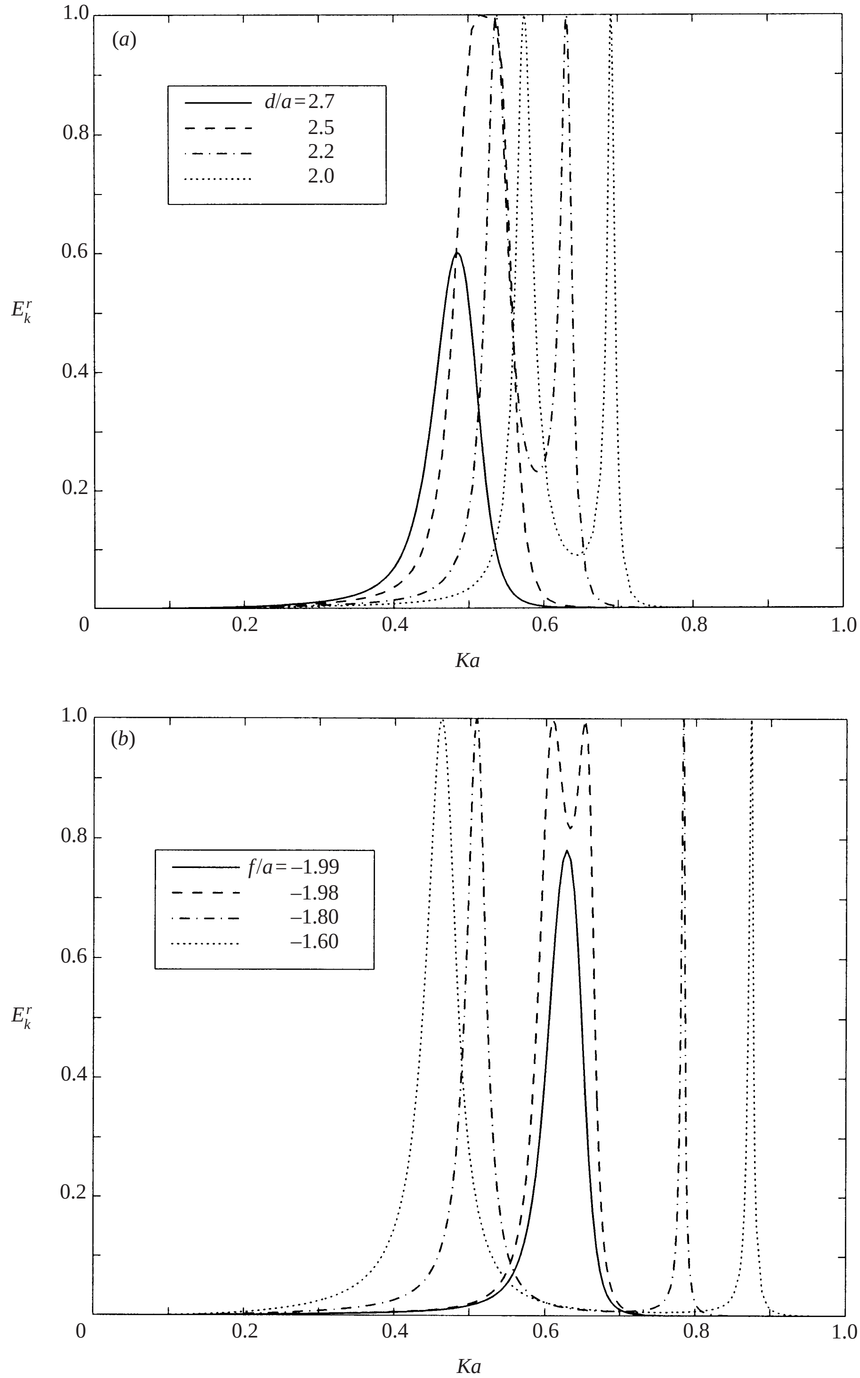

FIGURE 6. Reflection energies due to a wave of wavenumber k incident on a cylinder in the lower layer; $\rho = 0.5$ and $\alpha_{\text{inc}} = 0.34$: ($a$) $f/a = -1.95$, (b) $d/a = 2.0$.

4. Cylinder in the upper fluid

We now consider the case of a cylinder positioned in the upper fluid layer, $f/a > 1$. Polar coordinates are again defined via (3.1) and suitable multipoles take the form

$$\phi_n^{Is} = K_n(lr)\cos n\theta + \int_0^\infty \cosh nu \cos(lx\sinh u)[A_{Un}^{(0)}(u)\mathrm{e}^{vz} + B_{Un}^{(0)}(u)\mathrm{e}^{-vz}]\,\mathrm{d}u, \quad (4.1)$$

$$\phi_n^{IIs} = \int_0^\infty \cosh nu \cos(lx\sinh u)\mathrm{e}^{vz} C_{Un}^{(0)}(u)\,\mathrm{d}u, \quad (4.2)$$

$$\phi_n^{Ia} = K_n(lr)\sin n\theta + \int_0^\infty \sinh nu \sin(lx\sinh u)[A_{Un}^{(1)}(u)\mathrm{e}^{vz} + B_{Un}^{(1)}(u)\mathrm{e}^{-vz}]\,\mathrm{d}u, \quad (4.3)$$

$$\phi_n^{IIa} = \int_0^\infty \sinh nu \sin(lx\sinh u)\mathrm{e}^{vz} C_{Un}^{(1)}(u)\,\mathrm{d}u, \quad (4.4)$$

where

$$A_{Un}^{(q)}(u) = (v+K)\mathrm{e}^{-2vd}[(-1)^{n+q+1}(v-K\sigma)\mathrm{e}^{vf} - (v-K)\mathrm{e}^{-vf}]/(v-K)h(v), \quad (4.5)$$

$$B_{Un}^{(q)}(u) = [(-1)^{n+q+1}(v+K)\mathrm{e}^{v(f-2d)} - (v-K)\mathrm{e}^{-vf}]/h(v), \quad (4.6)$$

$$C_{Un}^{(q)}(u) = K(1-\sigma)B_{Un}^{(q)}(u)/(v-K). \quad (4.7)$$

We note that the functions (4.5)–(4.7) are the same as (4.7)–(4.9) in LM with u replaced by $v\,(= l\cosh u)$. When $l < K$, the multipoles have poles at $u = \gamma_1$ and $u = \gamma_2$, defined by (3.10) as before, whereas for $l > K$ there is only one pole at $u = \gamma_2$.

The far-field form of these multipoles, in the lower fluid layer, is given by

$$\phi_n^{IIs} \sim \pi\mathrm{i}(C_{Un}^{(0)\gamma_1}\cosh n\gamma_1 \mathrm{e}^{\pm\mathrm{i}\beta x}\mathrm{e}^{Kz} + C_{Un}^{(0)\gamma_2}\cosh n\gamma_2 \mathrm{e}^{\pm\mathrm{i}bx}\mathrm{e}^{kz}), \quad (4.8)$$

$$\phi_n^{IIa} \sim \pm\pi(C_{Un}^{(1)\gamma_1}\sinh n\gamma_1 \mathrm{e}^{\pm\mathrm{i}\beta x}\mathrm{e}^{Kz} + C_{Un}^{(1)\gamma_2}\sinh n\gamma_2 \mathrm{e}^{\pm\mathrm{i}bx}\mathrm{e}^{kz}), \quad (4.9)$$

as $x \to \pm\infty$, where

$$C_{Un}^{(q)\gamma_1} = \frac{(-1)^{n+q+1}2K(1-\sigma)\mathrm{e}^{K(f-2d)}}{\beta(2\mathrm{e}^{-2Kd} - 1 + \sigma)} \quad (4.10)$$

and

$$C_{Un}^{(q)\gamma_2} = \frac{K(1-\sigma)[(-1)^{n+q+1}(k+K)\mathrm{e}^{k(f-2d)} - (k-K)\mathrm{e}^{-kf}]}{b(k-K)[(1-2d(k+K))\mathrm{e}^{-2kd} - 1]}. \quad (4.11)$$

The polar expansions of the multipoles are

$$\phi_n^{Is} = K_n(lr)\cos n\theta + \sum_{m=0}^{\infty} B_{nm}^s I_m(lr)\cos m\theta, \quad (4.12)$$

$$\phi_n^{Ia} = K_n(lr)\sin n\theta + \sum_{m=1}^{\infty} B_{nm}^a I_m(lr)\sin m\theta, \quad (4.13)$$

where

$$B_{nm}^s = \epsilon_m \int_0^\infty \cosh mu\,\cosh nu\,((-1)^m A_{Un}^{(0)}(u)\mathrm{e}^{vf} + B_{Un}^{(0)}(u)\mathrm{e}^{-vf})\,\mathrm{d}u, \quad (4.14)$$

$$B_{nm}^a = 2\int_0^\infty \sinh mu\,\sinh nu\,((-1)^{m+1} A_{Un}^{(1)}(u)\mathrm{e}^{vf} + B_{Un}^{(1)}(u)\mathrm{e}^{-vf})\,\mathrm{d}u. \quad (4.15)$$

Incident wavenumber K

The potential ϕ_K can again be expanded using (3.21), in which the incident wave is given by (3.20) as before, but we now use the multipole expansions developed for the upper fluid layer, (4.1)–(4.4). After applying the body boundary condition, $\partial\phi_K/\partial r = 0$ on $r = a$, we obtain exactly the same systems of equations for α_n and β_n as before, (3.22) and (3.23), except with A^a_{mn} and A^s_{mn} replaced by B^a_{mn} and B^s_{mn}, respectively. These equations were solved by truncating to 4×4 systems to produce the results presented below. The accuracy achieved with this truncation parameter was three decimal places.

The transmission and reflection coefficients can extracted from the far-field form of the potential ϕ_K. Using (3.21), (4.8) and (4.9) with (3.24) we obtain

$$T_K = 1 + \pi \sum_{m=0}^{\infty} (\alpha_m C^{(1)\gamma_1}_{Um} \sinh m\gamma_1 + \mathrm{i}\beta_m C^{(0)\gamma_1}_{Um} \cosh m\gamma_1), \tag{4.16}$$

$$R_K = \pi \sum_{m=0}^{\infty} (-\alpha_m C^{(1)\gamma_1}_{Um} \sinh m\gamma_1 + \mathrm{i}\beta_m C^{(0)\gamma_1}_{Um} \cosh m\gamma_1), \tag{4.17}$$

$$t_K = \pi \sum_{m=0}^{\infty} (\alpha_m C^{(1)\gamma_2}_{Um} \sinh m\gamma_2 + \mathrm{i}\beta_m C^{(0)\gamma_2}_{Um} \cosh m\gamma_2), \tag{4.18}$$

$$r_K = \pi \sum_{m=0}^{\infty} (-\alpha_m C^{(1)\gamma_2}_{Um} \sinh m\gamma_2 + \mathrm{i}\beta_m C^{(0)\gamma_2}_{Um} \cosh m\gamma_2). \tag{4.19}$$

Incident wavenumber k

For this problem ϕ_{inc} is given, in the upper fluid, by $\exp(\mathrm{i}bx)g(z)$, where $g(z)$ is defined in (2.12). The polar expansion is

$$\phi^I_{\mathrm{inc}} = \frac{1}{K(\sigma-1)} \sum_{m=0}^{\infty} \epsilon_m I_m(lr)[((-1)^m \mathrm{e}^{kf}(K\sigma - k) + \mathrm{e}^{-kf}(K-k)) \cos m\theta \cosh m\gamma \\ + \mathrm{i}((-1)^{m+1} \mathrm{e}^{kf}(K\sigma - k) + \mathrm{e}^{-kf}(K-k)) \sin m\theta \sinh m\gamma], \tag{4.20}$$

where $\cosh\gamma = k/l = 1/\sin\alpha_{\mathrm{inc}}$. The velocity potential ϕ_k is expanded as in (3.21), where ϕ^s_m and ϕ^a_m are the symmetric and antisymmetric multipoles developed for the upper fluid. After application of the body boundary condition we obtain the equations

$$\alpha_n + Z_n \sum_{m=1}^{\infty} \alpha_m B^a_{mn} = \frac{2\mathrm{i}Z_n}{K(\sigma-1)}((-1)^n \mathrm{e}^{kf}(K\sigma - k) - \mathrm{e}^{-kf}(K-k)) \sinh n\gamma, \tag{4.21}$$

$$\beta_n + Z_n \sum_{m=0}^{\infty} \beta_m B^s_{mn} = \frac{\epsilon_n Z_n}{K(\sigma-1)}((-1)^{n+1} \mathrm{e}^{kf}(K\sigma - k) - \mathrm{e}^{-kf}(K-k)) \cosh n\gamma. \tag{4.22}$$

The expressions for R_k and r_k are the same as those for R_K and r_K given, respectively, by (4.17) and (4.19). For the transmission coefficients we have

$$T_k = \pi \sum_{m=0}^{\infty} (\alpha_m C^{(1)\gamma_1}_{Um} \sinh m\gamma_1 + \mathrm{i}\beta_m C^{(0)\gamma_1}_{Um} \cosh m\gamma_1), \tag{4.23}$$

$$t_k = 1 + \pi \sum_{m=0}^{\infty} (\alpha_m C^{(1)\gamma_2}_{Um} \sinh m\gamma_2 + \mathrm{i}\beta_m C^{(0)\gamma_2}_{Um} \cosh m\gamma_2). \tag{4.24}$$

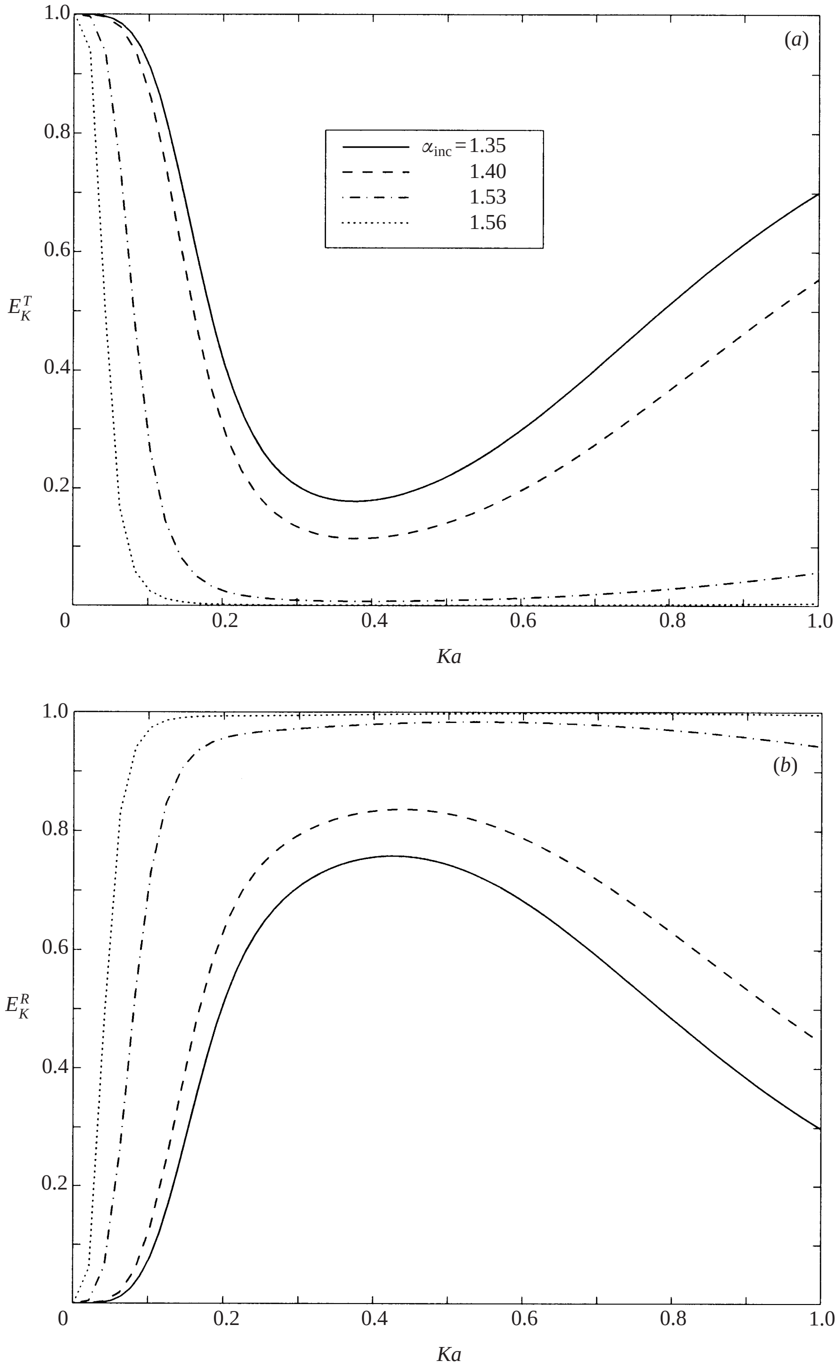

FIGURE 7. (a) Transmission and (b) reflection energies due to a wave of wavenumber K incident on a cylinder in the upper layer; $\rho = 0.5$, $d/a = 2.5$ and $f/a = 1.25$.

Results

Figures 7–8 show the reflection and transmission energies for an incident wave of wavenumber K (a free-surface mode) on a cylinder submerged in the upper fluid layer. The submergence of the cylinder f/a is fixed at 1.25, the depth d/a of the upper

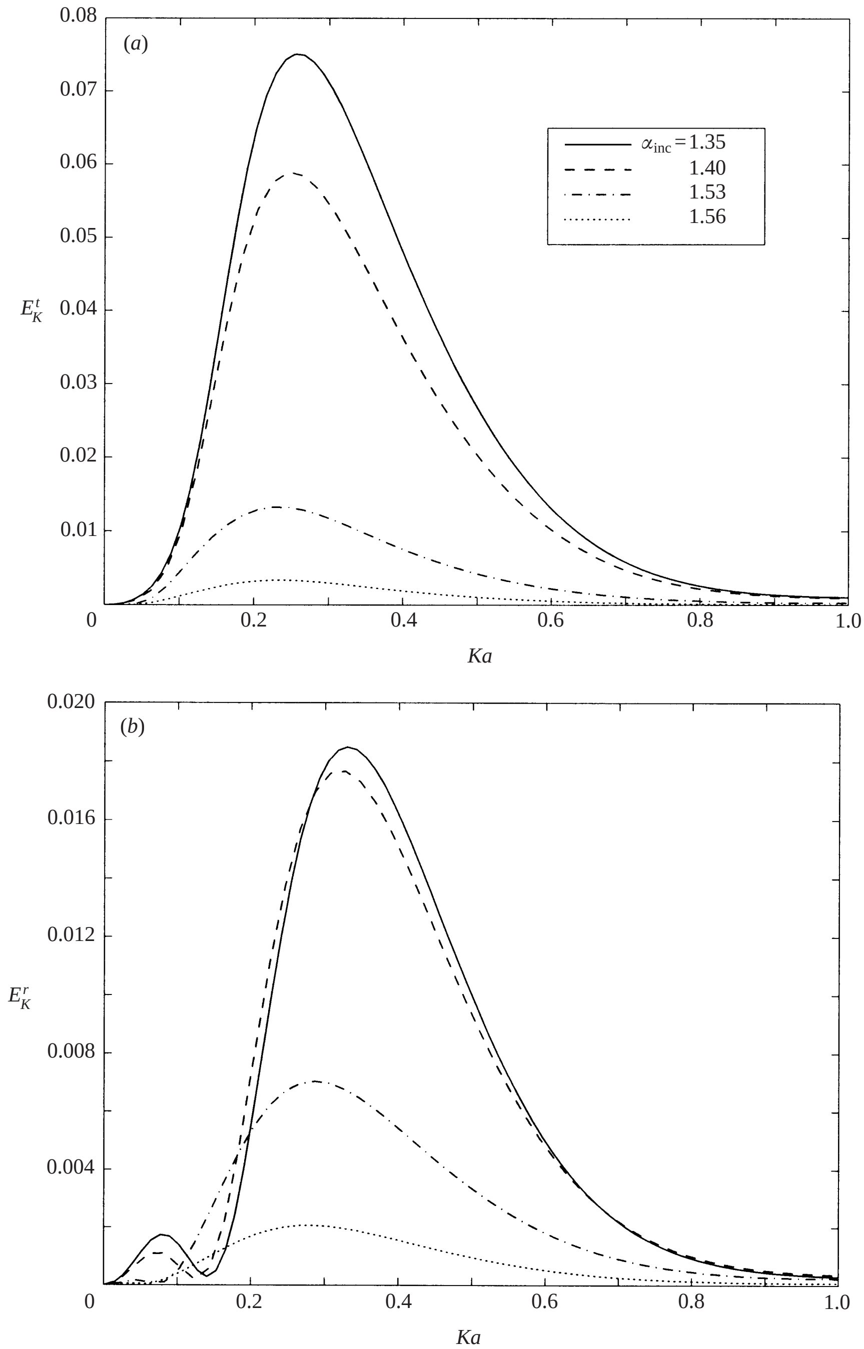

FIGURE 8. (a) Transmission and (b) reflection energies due to a wave of wavenumber K incident on a cylinder in the upper layer; $\rho = 0.5$, $d/a = 2.5$ and $f/a = 1.25$.

fluid layer is 2.5 and the density ratio ρ is 0.5. The different curves correspond to four different angles of incidence, $\alpha_{\rm inc} = 1.35$, 1.4, 1.53 and 1.56. These angles are same as those used in figures 2 and 3. The results are similar to those for the scattering of an incident wave of wavenumber K by a cylinder in the lower fluid layer and display the same trends.

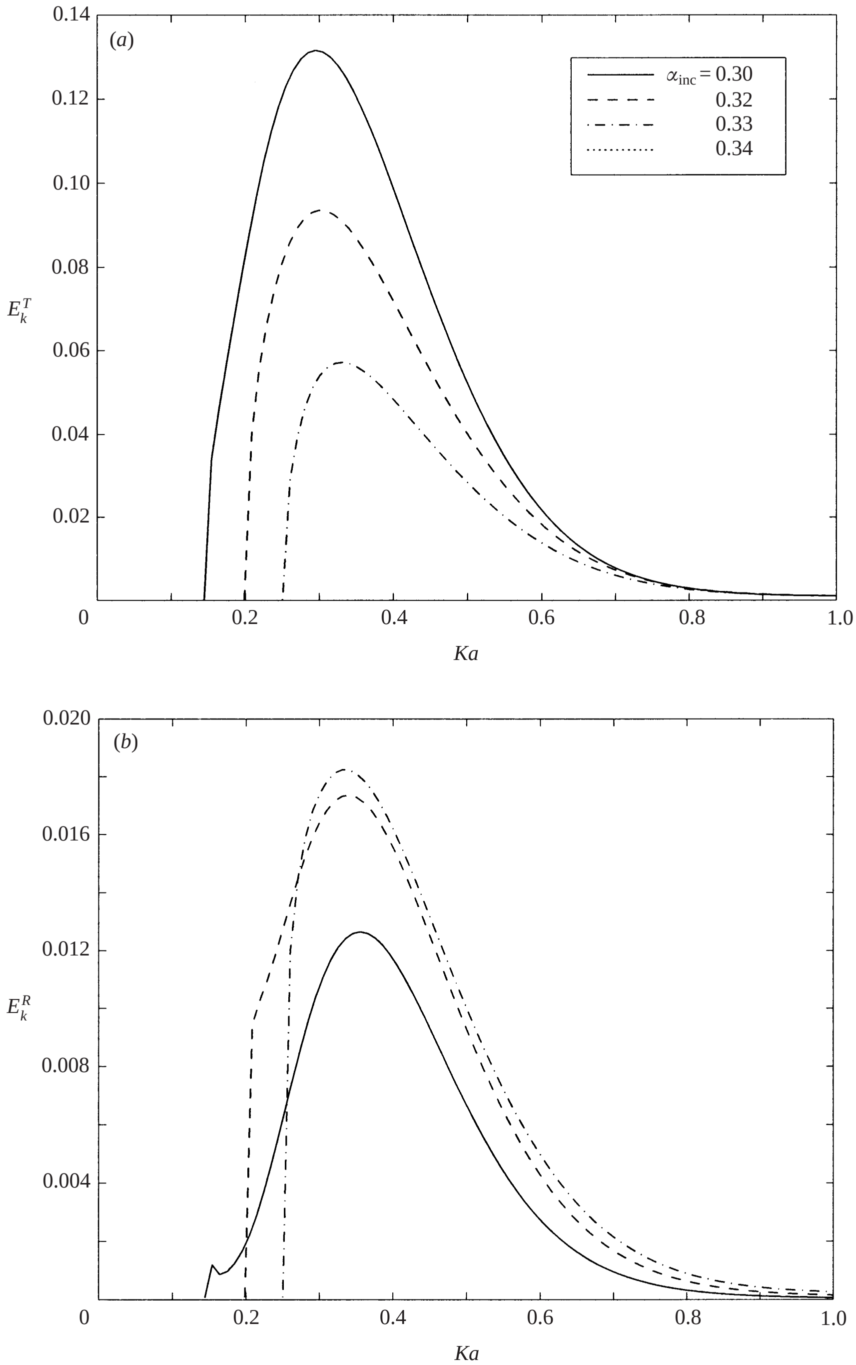

FIGURE 9. (a) Transmission and (b) reflection energies due to a wave of wavenumber k incident on a cylinder in the upper layer; $\rho = 0.5$, $d/a = 2.5$ and $f/a = 1.25$.

Figures 9 and 10 show reflection and transmission energies of an incident wave of wavenumber k (an interfacial mode) on a cylinder submerged in the upper fluid layer. The parameter settings are the same as in figures 7 and 8 and the different curves correspond to $\alpha_{inc} = 0.3$, 0.32, 0.33 and 0.34. The critical angle α_c is 0.3398

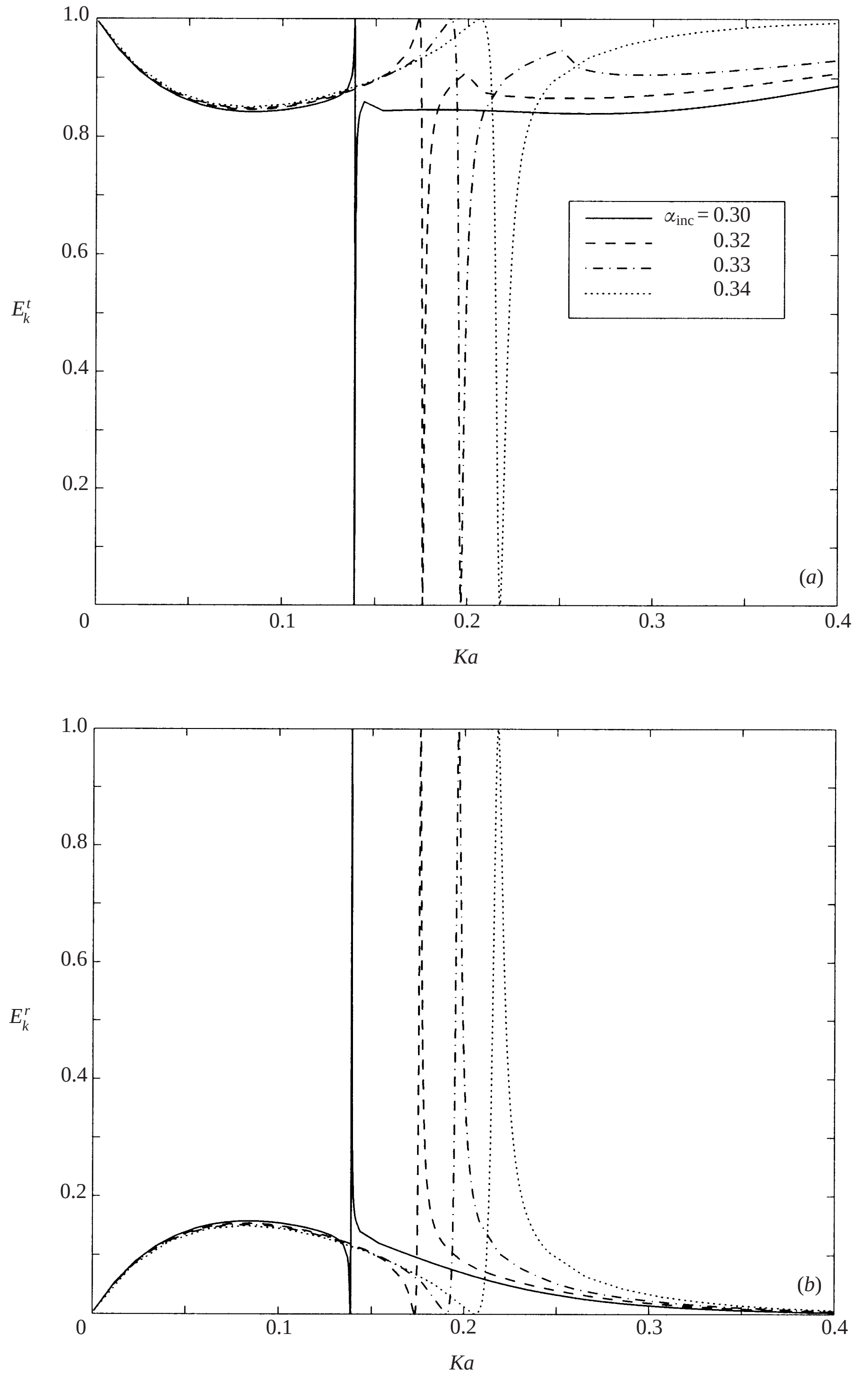

FIGURE 10. (*a*) Transmission and (*b*) reflection energies due to a wave of wavenumber k incident on a cylinder in the upper layer; $\rho = 0.5$, $d/a = 2.5$ and $f/a = 1.25$.

and the cut-off frequencies for the first three angles are $K_c a \approx 0.144$, 0.198 and 0.250, respectively. Again there are similarities with the case of the cylinder in the lower fluid shown in figures 4 and 5. Energy conversion between wavenumbers only occurs for frequencies greater than the cut-off frequency as shown in figures 9(*a*) and 9(*b*).

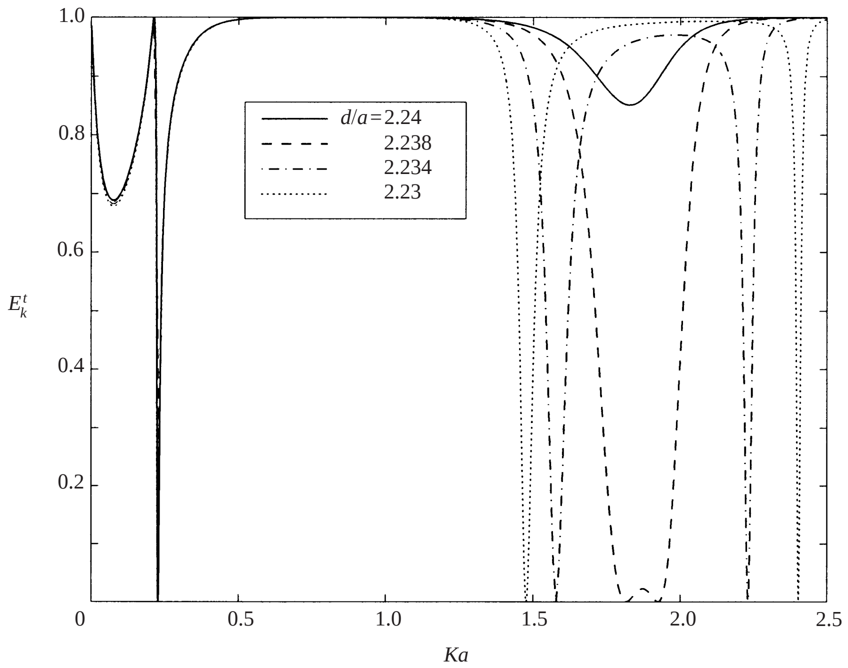

FIGURE 11. Transmission energies due to a wave of wavenumber k incident on a cylinder in the upper layer; $\rho = 0.5$, $d/f = 2$ and $\alpha_{\text{inc}} = 0.35$.

Figures 10(a) and 10(b) show the transmitted and reflected energies at the incident wavenumber. There is a zero of transmission occurring before the cut-off frequency. However, unlike in the case shown in figures 5(a) and 5(b), we have a point of total transmission preceding this. As the angle of incidence is increased the frequencies of these pairs of zero and total transmission increase and also separate.

More than one zero of transmission may occur for a given geometry. This is illustrated in figure 11 which shows the transmission energies E_k^t for an incident wave of wavenumber k with angle $\alpha_{\text{inc}} = 0.35$, which is greater than the critical angle. The ratio of the depth of the upper fluid layer to the submergence of the cylinder is fixed at $d/f = 2$ so that the cylinder is always halfway between the interface and the free surface. The different curves correspond to the values $d/a = 2.24$, 2.238, 2.234 and 2.23. For all the curves there is a frequency of total transmission at $Ka \approx 0.213$ followed immediately by a zero of transmission at $Ka \approx 0.227$. When $d/a = 2.24$ we have a local minimum at $Ka \approx 1.825$ and as the depth of the upper fluid layer is decreased, bringing the free surface and interface closer to the surface of the cylinder, we obtain another zero of transmission. As the depth is decreased further this splits and we obtain a total of three zeros of transmission.

If we let $\rho \to 0$ in this problem then the multipoles defined by (4.1) and (4.3) go over to the single-layer multipoles for finite depth (given in Linton & McIver 2001, for example). Thus by letting $\rho \to 0$ we can recover the results for the scattering of oblique waves by a horizontal circular cylinder in finite water depth.

5. Conclusion

In this paper we have studied the problem of oblique wave scattering by horizontal cylinders in two-layer fluids using linear water wave theory. The upper layer is of finite thickness and is bounded above by a free surface and below by an infinite layer of fluid of greater density. In this situation waves can propagate at two different wavenumbers for the same frequency, one of which corresponds to a free-surface disturbance and the other to an interfacial wave motion. When the incident wave is on the free surface we always find energy transfer to the interface, but for incident interfacial waves there are parameter ranges for which no energy transfer to the free surface is possible.

We have analysed the scattering problem of oblique waves by a horizontal circular cylinder submerged in either the upper or lower layer of a two-layer fluid using multipole expansions. When the cylinder is positioned in the lower fluid layer and waves are normally incident upon it, it was shown in LM that all the energy is transmitted. We have shown that this is not true for oblique waves. We have found that for oblique waves incident along the interface when a cylinder is in either fluid layer there are isolated frequencies at which all the incident energy is reflected.

REFERENCES

Barthélemy, E., Kabbaj, A. & Germain, J.-P. 2000 Long surface wave scattered by a step in a two-layer fluid. *Fluid Dyn. Res.* **26**, 235–255.

Cadby, J. R. & Linton, C. M. 2000 Three-dimensional water-wave scattering in two-layer fluids. *J. Fluid Mech.* **423**, 155–173.

Gavrilov, N., Ermanyuk, E. & Sturova, I. 1999 Scattering of internal waves by a circular cylinder submerged in a stratified fluid. In *Proc. 22nd Symposium on Naval Hydrodynamics, ONR*, pp. 907–919.

Lamb, H. 1932 *Hydrodynamics* (6th Edn). Cambridge University Press. Reprinted 1993.

Levine, L. 1965 Scattering of surface waves by a submerged circular cylinder. *J. Math. Phys.* **6**, 1231–1243.

Linton, C. M. & McIver, M. 1995 The interaction of waves with horizontal cylinders in two-layer fluids. *J. Fluid Mech.* **304**, 213–229 (referred to herein as LM).

Linton, C. M. & McIver, P. 2001 *Handbook of Mathematical Techniques for Wave/Structure Interactions.* Chapman & Hall/CRC, Boca Raton.

Stokes, G. G. 1847 On the theory of oscillatory waves. *Trans. Camb. Phil. Soc.* **8**, 441–455. Reprinted in *Mathematical and Physical Papers*, vol. 1, pp. 314–326. Cambridge University Press.

Sturova, I. V. 1994*a* Planar problem of hydrodynamic shaking of a submerged body in the presence of motion in a two-layered fluid. *J. Appl. Mech. Tech. Phys.* **35**, 670–679.

Sturova, I. V. 1994*b* Plane problem of hydrodynamic rocking of a body submerged in a two-layer fluid without forward speed. *Fluid Dyn.* **29**, 414–423.

Sturova, I. V. 1999 Problems of radiation and diffraction for a circular cylinder in a stratified fluid. *Fluid Dyn.* **34**, 521–533.

Ursell, F. 2001 The local expansion of a source of oblique water waves in the free surface. *Wave Motion* **33**, 109–116.

Yeung, R. W. & Nguyen, T. 1999 Radiation and diffraction of waves in a two-layer fluid. In *Proc. 22nd Symposium on Naval Hydrodynamics, ONR*, pp. 875–891.

Zilman, G., Kagan, L. & Miloh, T. 1996 Hydrodynamics of a body moving over a mud layer – Part II: Added-mass and damping coefficients. *J. Ship Res.* **40**, 39–45.

Zilman, G. & Miloh, T. 1995 Hydrodynamics of a body moving over a mud layer – Part I: Wave resistance. *J. Ship Res.* **39**, 194–201.